THE JOURNAL OF PHYSICAL CHEMISTRY C

Article

pubs.acs.org/JPCC

# DFT-D3 Study of Some Molecular Crystals

Jonas Moellmann and Stefan Grimme*

Mulliken Center for Theoretical Chemistry, Institut für Physikalische und Theoretische Chemie der Universität Bonn, Beringstr. 4, D-53115 Bonn, Germany

Supporting Information

**ABSTRACT:** We investigate the performance of the dispersion correction D3 with and without an explicit three-body dispersion term for the energetic and structural properties of rare gas and molecular crystals. Therefore, the two- and three-body gradient of the dispersion energy is implemented in the periodic plane-wave program VASP. It is combined with different density functionals at the level of the general gradient approximation (GGA) and hybrid functionals. Cohesive energies and lattice parameters for the rare gas crystals Ar, Kr, and Xe and a set of 23 molecular crystals are calculated and compared to experimental reference values. In general, all tested methods yield very good results. For the molecular crystals the mean absolute deviation of lattice energies from reference data (about 1−2 kcal/mol) is close to or below their uncertainties. The influence of the three-body Axilrod−Teller−Muto dispersion term on energy and structure is found to be rather small. While on a GGA level cohesive energies become slightly worse, for hybrid functionals the three-body term improves the results.

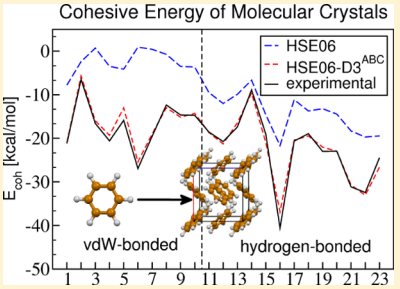


## INTRODUCTION

It is well-known that approximate standard density functionals (DFs) in electronic structure theory lack a proper description for long-range London dispersion interactions.[1−3] In recent years a variety of different correction schemes have been developed that attempt to fix this shortcoming,[4−7] which is of particular importance for the application of density functional theory (DFT) in condensed phase simulations. Several benchmarks with accurate reference values have validated the good performance of our DFT-D3 method[8] for noncovalent interactions in small as well as large systems in the gas phase.[9,10] Most molecular quantum chemistry codes have implemented at least one dispersion correction, and they should be used by default for all DFT calculations. The importance of a proper description of dispersion interaction in molecular crystals, e.g., for crystal structure and polymorph prediction, has been pointed out.[11−13] Compared to the molecular case for which the quantum chemistry "golden standard" CCSD(T)/CBS can be readily applied, for periodic systems the quest how to obtain good reference data appears. The results of experimental measurements are not directly comparable with quantum chemical calculations because they include vibrational and thermal contributions which are cumbersome to approximate by theory.

Recently Otero-dela-Roza and Johnson developed a benchmark set of lattice energies for common organic crystals which are based on experimental reference data to evaluate the performance of theoretical methods.[14] They corrected experimental sublimation enthalpies back to zero-point energy exclusive electronic lattice energies ($E_{coh}$). This test set was extended, and the reference values were refined by Reilly and Tkatchenko.[15,16] The extended test set is used here together with well-known data for rare gas crystals to evaluate the performance of the DFT-D3 method for periodic systems.

This paper concentrates on the implementation of the DFT-D3 correction into the periodic DFT program VASP and its performance for noncovalently bound periodic systems. In particular we describe for the first time the implementation of the Axilrod−Teller−Muto (ATM[17,18]) three-body dispersion term and its analytical gradient for the atomic positions and cell vectors for periodic systems and a thorough test of its importance. Because detailed information on the performance of GGA versus hybrid functionals is lacking, we investigate this aspect by employing PBE0-D3 and HSE06-D3 here for the first time in this context. For recent related applications on dispersion-corrected DFT to molecular crystals including full optimization and/or many-body dispersion effects see refs 19−23.

## THEORY

The pairwise DFT-D3 dispersion energy with the standard Becke−Johnson (BJ)[24,25] damping for periodic systems is given by

$$E_{\mathrm{disp}} = \sum_{\mathrm{AB}} \sum_{n=6,8} \sum_{\mathbf{T}} \frac{C_n^{\mathrm{AB}}}{(|\mathbf{r}_{\mathrm{AB}} + \mathbf{T}|)^n + (a_1 R_0^{\mathrm{AB}} + a_2)} \quad (1)$$

where the sum is over all atom pairs AB; $C_n^{\mathrm{AB}}$ is the isotropic dispersion coefficient of the $n$th order; and $\mathbf{r}_{\mathrm{AB}}$ is the distance vector between the two atoms. The $a_1 R_0^{\mathrm{AB}} + a_2$ term represents the damping at short interatomic distances so that the

Received: February 4, 2014
Revised: March 13, 2014
Published: March 13, 2014



   dx.doi.org/10.1021/jp501237c | J. Phys. Chem. C 2014, 118, 7615−7621

dispersion energy becomes constant as required by theory.[26] The summation over all unit cells in real space is done by adding all unit cell translation vectors $\mathbf{T}$ to $\mathbf{r}_{AB}$ within a cutoff sphere (usually with a radius of $r_{Cutoff}$ = 50 Å).

The derivatives for the atomic positions in the Cartesian coordinate system can be written in this way

$$\frac{\partial E_{disp}}{\partial x_A} = \sum_B \sum_{\mathbf{T}} \frac{\partial E_{disp}}{\partial |\mathbf{r}_{AB} + \mathbf{T}|} \times \frac{\partial |\mathbf{r}_{AB} + \mathbf{T}|}{\partial x_A} \tag{2}$$

where $x_A$ is one Cartesian component of atom A. The cell gradient it is conveniently calculated from the stress tensor. The Cartesian stress tensor $\sigma$ is a 3 × 3 matrix

$$\sigma = \begin{pmatrix} \sigma_{x,x} & \sigma_{x,y} & \sigma_{x,z} \\ \sigma_{y,x} & \sigma_{y,y} & \sigma_{y,z} \\ \sigma_{z,x} & \sigma_{z,y} & \sigma_{z,z} \end{pmatrix} \tag{3}$$

where each element is defined by

$$\sigma_{x,y} = \sum_{AB} \sum_{n=6,8} \sum_{\mathbf{T}} \frac{\partial E_{disp}}{\partial |\mathbf{r}_{AB} + \mathbf{T}|} \times \frac{\delta x_{AB} \delta y_{AB}}{|\mathbf{r}_{AB} + \mathbf{T}|} \tag{4}$$

Here, $\delta x_{AB}$ and $\delta y_{AB}$ are the differences of the Cartesian components of the positions of the atoms A and B. From the terms $(\partial E_{disp})/(\partial |\mathbf{r}_{AB} + \mathbf{T}|)$ the Cartesian gradient for the atomic positions as well as the cell gradient are easily obtained.

The calculation of these terms requires an additional summation over all atoms, since the $C_{AB}^n$ coefficient in the D3 method depends on the coordination numbers $CN_A$ and $CN_B$, which in turn depend on the distances to all other atoms. So the full gradient with respect to a specific distance $|\mathbf{r}_{AB} + \mathbf{T}|$ reads

$$\frac{\partial E_{disp}}{|\mathbf{r}_{AB} + \mathbf{T}|} = \sum_{n=6,8} \frac{\partial}{\partial |\mathbf{r}_{AB} + \mathbf{T}|} \left( \frac{C_n^{AB}}{(|\mathbf{r}_{AB} + \mathbf{T}|)^n + (a_1 R_0^{AB} + a_2)} \right) \tag{5}$$

$$+ \sum_{C \neq A,B} \sum_{n=6,8} \left( \frac{1}{(|\mathbf{r}_{AC} + \mathbf{T}|)^n + (a_1 R_0^{AC} + a_2)} \right) \frac{\partial C_{AC}^n}{\partial |\mathbf{r}_{AB} + \mathbf{T}|} \tag{6}$$

$$+ \sum_{n=6,8} \left( \frac{1}{(|\mathbf{r}_{BC} + \mathbf{T}|)^n + (a_1 R_0^{BC} + a_2)} \right) \frac{\partial C_{BC}^n}{\partial |\mathbf{r}_{AB} + \mathbf{T}|} \tag{7}$$

To calculate the gradient for all atomic coordinates requires a triply nested loop over all atoms, and therefore the calculation scales with $O(N^3)$ with respect to the system size.

The periodic ATM-three-body term[17,18] is defined as

$$E_{abc} = \sum_{ABC} \sum_{\mathbf{T}_B} \sum_{\mathbf{T}_C} \frac{C_9^{ABC}(3 \cos\alpha \cos\beta \cos\gamma + 1)}{(r_{AB} r_{BC} r_{CA})^3} \cdot f_{9,damp}(r_{AB}, r_{BC}, r_{AC}) \tag{8}$$

where $\alpha,\beta,\gamma$ are the internal angles of the atom triple ABC; $r_{AB} = |\mathbf{r}_{AB} + \mathbf{T}_B|$, $r_{BC} = |\mathbf{r}_{BC} + \mathbf{T}_C - \mathbf{T}_B|$, and $r_{CA} = |\mathbf{r}_{CA} - \mathbf{T}_C|$ are the distances between the atoms ABC; and $C_9^{ABC}$ is the triple dipole constant, which is approximated by $C_9^{ABC} = (C_6^{AB} C_6^{BC} C_6^{CA})^{1/2}$ in the DFT-D3 method. The damping function $(f_{9,damp})$ which prevents singularities for short interatomic distances, is the one used in the original D3 paper. It is a so-called zero-damping function that employs the geometric average of the three distances as an argument. The generally small influence of different damping schemes is discussed in detail in ref 19. For details of the implemented three-body term see ref 8.

The derivative can be separated in a similar manner as follows

$$\frac{\partial E_{abc}}{\partial |\mathbf{r}_{AB} + \mathbf{T}_B|} = \sum_{BC} \sum_{\mathbf{T}_C} \frac{\partial}{\partial |\mathbf{r}_{AB} + \mathbf{T}_B|} \left( C_9^{ABC} \frac{(3 \cos\alpha \cos\beta \cos\gamma + 1)}{(r_{AB} r_{BC} r_{CA})^3} \right) \tag{9}$$

$$+ \sum_{D \neq A,B,C} \sum_{\mathbf{T}_D} \left( \frac{(3 \cos\beta \cos\gamma \cos\delta + 1)}{(r_{BC} r_{CD} r_{BD})^3} \right) \frac{\partial C_9^{BCD}}{\partial |\mathbf{r}_{AB} + \mathbf{T}_B|} \tag{10}$$

$$+ \sum_{D \neq A,B,C} \sum_{\mathbf{T}_D} \left( \frac{(3 \cos\alpha \cos\gamma \cos\delta + 1)}{(r_{AC} r_{CD} r_{AD})^3} \right) \frac{\partial C_9^{ACD}}{\partial |\mathbf{r}_{AB} + \mathbf{T}_B|} \tag{11}$$

Since the triple dipole constants $C_9^{ACD}$ and $C_9^{BCD}$ depend on the term $|\mathbf{r}_{AB} + \mathbf{T}_B|$ via the $C_6^{AC}$, $C_6^{AD}$, $C_6^{BC}$, and $C_6^{BD}$ coefficients, the calculation of the gradient scales with $O(N^4)$. Because this increases the computational time substantially, the necessity of the ATM computation should be investigated carefully.

## COMPUTATIONAL DETAILS

All periodic calculations have been performed with the plane-wave DFT program VASP (v5.3)[27] using the PAW-potentials[28,29] for the description of the core electrons. A very large basis with a cutoff of 1000 eV was used for all calculations. The reciprocal space was covered by a Γ-centered Monkhorst−Pack lattice of 4 × 4 × 4 K-points. The convergence criteria were set to $10^{-6}$ eV for the SCF and 0.005 eV/Å for the geometry optimization. Starting from the experimental X-ray structure, all atomic positions as well as the unit cell were optimized. The (meta)GGA functionals PBE[30] and TPSS[31] as well as the hybrid functionals PBE0[32] and HSE06[33] as implemented in VASP were used.[34] As an approximation for isolated (gas-phase) molecules, a unit cell was used which is large enough to separate the molecule by at least 14 Å from any of its neighbors.

Special attention is paid to the implementation of the ATM three-body interaction. The calculation of atom pairs and triples is conducted in real space within a certain cutoff. For the pair contribution a cutoff of 50 Å was found to be sufficient. For the triple contribution a smaller cutoff of ∼21 Å (40 Bohr) covers more than 99% of the three-body energy compared to a larger cutoff of 50 Å. The use of the smaller cutoff reduces the computational time roughly by a factor of 100, which becomes noticeable for the calculation of the gradient. Since the ATM term is only about 5% of the total dispersion contribution to the binding energy (about 1 kcal mol$^{-1}$ for typical molecular crystals), a very small error of <0.01 kcal mol$^{-1}$ can be estimated for this truncation.

Dispersion-corrected functionals are labeled with the suffix "-D3" (e.g., DFT-D3). When the three-body contribution is also considered the suffix is "-D3$^{ABC}$". If geometry optimizations are carried out, the forces of the three-body contribution are


dx.doi.org/10.1021/jp501237c | J. Phys. Chem. C 2014, 118, 7615−7621

also considered, and the system is fully relaxed at the D3$^{ABC}$ level.

New D3 damping parameters for the range-separated hybrid functional HSE06[33,34] were developed on the basis of a fit for the standard benchmark set S66,[10] and values of $a1$ = 0.383, $a2$ = 5.685, and $s8$ = 2.310 similar to those for PBE0 were obtained.

The cohesive energy (given always in kcal mol$^{-1}$ per molecule) is computed as

$$E_{coh} = \frac{E_{solid}}{N} - E_{gas} \quad (12)$$

where $N$ is the number of molecules per unit cell.

## RESULTS AND DISCUSSION

The first test of the implemented dispersion correction including the three-body term was performed on noble gas crystals of Ar, Kr, and Xe, which are archetypical noncovalent crystals, held together purely by van der Waals (vdW) interactions. The unit cell, consisting of only one atom, was optimized, and also a potential energy scan with different lattice parameters was performed to find the optimal lattice constant. Additionally via a Murnhagan equation-of-state,[35] the Bulk modulus and the cohesive energy ($E_{coh}$) were determined. These values are compared with the results of the recently proposed PBE-TS+SCS method.[21] In this work experimental data were corrected to pure electronic contributions of each property which are used here for comparison.

In Table 1 the results for lattice constants, cohesive energies, and bulk moduli are listed. The performance of all tested dispersion-corrected functionals is very similar, and the results are all in very good agreement with the experimental reference data. In general the computed lattice constants are slightly too large; the bulk moduli are too shallow; and the cohesive binding is too strong for most of the tested functionals.

Statistical mean absolute deviations (MADs) over all four cases are listed in Table 2. The mean deviations (MDs) in lattice constants are between 0.05 and 0.3 Å, where BLYP-D3 performs best and TPSS-D3 has the largest MAD. For the cohesive energy PBE-D3 and TPSS-D3 both perform similarly well with deviations of only 6−9 meV. BLYP-D3 overbinds by nearly 30 meV on average. The different dispersion corrections D3 and TS behave very similar. The bulk modulus, which is a nonequilibrium property, is generally underestimated by all functionals but BLYP-D3. HSE06-D3 gives the best results and deviates by only 0.5 GPa on average. TPSS-D3 results in the largest MAD of 0.94 GPa.

The three-body contribution has only a marginal impact on any of these properties. It contributes only about 2−4% to the dispersion energy. Its absolute contribution for Xe is 4 meV and even smaller for the lighter elements. Since its contribution to the energy is rather small, the influence on the lattice constant is even smaller, so one can safely neglect its contribution in optimizations of these or similar systems.

A larger test set for the performance of dispersion corrections is the X23 benchmark set, developed by Otero-dela-Rosa et al. and extended and refined by Tkatchenko.[14−16] It contains 23 crystal structures of small and medium sized molecules with 3−26 atoms. The molecules are depicted in Figure 1. The experimental sublimation enthalpies were back-corrected to pure electronic energies $E_{coh}$ which can be compared directly to the computed values.

**Table 1. Lattice Constants, Bulk Moduli, And Cohesive Energies for Rare Gas Crystals[a]**

| Ne | $a_0$ [Å] | $B_0$ [GPa] | $E_{coh}$ [meV] |
|---|---|---|---|
| ref | 4.46 | 1.17 | 20 |
| PBE-D3 | 4.45 | 2.00 | 37 |
| PBE-D3$^{ABC}$ | 4.46 | 1.97 | 36 |
| PBE-TS+SCS | 4.49 | 2.6 | 40 |
| BLYP-D3 | 4.59 | 0.76 | 8 |
| BLYP-D3$^{ABC}$ | 4.60 | 0.72 | 7 |
| TPSS-D3 | 4.65 | 1.49 | 29 |
| TPSS-D3$^{ABC}$ | 4.65 | 1.46 | 29 |
| HSE06-D3 | 4.49 | 1.38 | 26 |
| HSE06-D3$^{ABC}$ | 4.50 | 1.34 | 25 |
| Ar | $a_0$ [Å] | $B_0$ [GPa] | $E_{coh}$ [meV] |
| ref | 5.30 | 2.70 | 80 |
| PBE-D3 | 5.48 | 2.41 | 87 |
| PBE-D3$^{ABC}$ | 5.49 | 2.38 | 85 |
| PBE-TS+SCS | 5.60 | 2.8 | 80 |
| BLYP-D3 | 5.35 | 3.16 | 80 |
| BLYP-D3$^{ABC}$ | 5.36 | 3.09 | 78 |
| TPSS-D3 | 5.64 | 2.02 | 83 |
| TPSS-D3$^{ABC}$ | 5.65 | 2.00 | 81 |
| HSE06-D3 | 5.49 | 2.13 | 86 |
| HSE06-D3$^{ABC}$ | 5.50 | 2.09 | 84 |
| Kr | $a_0$ [Å] | $B_0$ [GPa] | $E_{coh}$ [meV] |
| ref | 5.65 | 3.60 | 116 |
| PBE-D3 | 5.85 | 2.52 | 116 |
| PBE-D3$^{ABC}$ | 5.86 | 2.48 | 114 |
| PBE-TS+SCS | 6.01 | 2.9 | 99 |
| BLYP-D3 | 5.67 | 4.45 | 141 |
| BLYP-D3$^{ABC}$ | 5.68 | 4.36 | 138 |
| TPSS-D3 | 5.98 | 2.15 | 120 |
| TPSS-D3$^{ABC}$ | 5.99 | 2.14 | 117 |
| HSE06-D3 | 5.80 | 2.59 | 133 |
| HSE06-D3$^{ABC}$ | 5.81 | 2.56 | 130 |
| Xe | $a_0$ [Å] | $B_0$ [GPa] | $E_{coh}$ [meV] |
| ref | 6.13 | 3.60 | 164 |
| PBE-D3 | 6.31 | 2.74 | 163 |
| PBE-D3$^{ABC}$ | 6.33 | 2.71 | 160 |
| PBE-TS+SCS | 6.48 | 3.0 | 132 |
| BLYP-D3 | 6.11 | 5.41 | 239 |
| BLYP-D3$^{ABC}$ | 6.12 | 5.29 | 235 |
| TPSS-D3 | 6.35 | 2.30 | 183 |
| TPSS-D3$^{ABC}$ | 6.37 | 2.29 | 180 |
| HSE06-D3 | 6.19 | 3.46 | 218 |
| HSE06-D3$^{ABC}$ | 6.21 | 3.39 | 214 |

[a]Reference and TS+SCS values from ref 21.

**Table 2. Average Deviations from Lattice Constants, Bulk Moduli, and Cohesive Energies for Rare Gas Crystals**

| MAD | $a_0$ [Å] | $B_0$ [GPa] | $E_{coh}$ [meV] |
|---|---|---|---|
| PBE-D3 | 0.14 | 0.77 | 6 |
| PBE-D3$^{ABC}$ | 0.15 | 0.78 | 7 |
| PBE-TS+SCS | 0.26 | 0.7 | 17 |
| BLYP-D3 | 0.05 | 0.88 | 28 |
| BLYP-D3$^{ABC}$ | 0.06 | 0.82 | 27 |
| TPSS-D3 | 0.27 | 0.94 | 9 |
| TPSS-D3$^{ABC}$ | 0.28 | 0.94 | 7 |
| HSE06-D3 | 0.11 | 0.48 | 21 |
| HSE06-D3$^{ABC}$ | 0.12 | 0.51 | 18 |


dx.doi.org/10.1021/jp501237c | J. Phys. Chem. C 2014, 118, 7615−7621

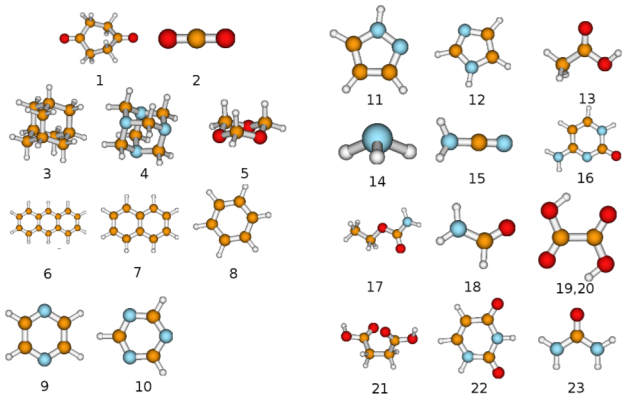


**Figure 1.** Molecules in the X23 test set. We use the colors brown for carbon, red for oxygen, and blue for nitrogen.

We tested the (meta-)GGA functionals PBE and TPSS, the hybrid functional PBE0, and the range-separated hybrid HSE06 together with the D3 dispersion correction. For the PBE and TPSS functionals the atomic positions and unit cell were fully optimized. For the hybrid functionals, full geometry optimizations are computationally too demanding, and hence for PBE0 and HSE06 only single-point calculations on the basis of TPSS-D3 geometries were performed.

The results for $E_{coh}$ are listed in Table 3. The MAD for all functionals is about 1 kcal mol$^{-1}$. There are slight differences between the functionals, but since the accuracy of the reference values was estimated to be about 0.7 kcal mol$^{-1}$, the performance of all methods is considered to be satisfactory. The MD and MAD values for all functionals are listed in Table 4. Since the uncorrected functionals result in mostly unbound crystals or $E_{coh}$ values far from the reference, only the results of dispersion-corrected functionals are discussed.

**Table 4. Mean Deviation (MD) and Mean Absolute Deviation (MAD) of Different Functionals for the X23 (All Values in kcal mol$^{-1}$)**

| functional | MD | MAD |
|---|---|---|
| PBE-D3 | −0.4 | 1.1 |
| PBE-D3$^{ABC}$ | 0.5 | 1.2 |
| PBE+MBD[a] | −1.1 | 1.4 |
| TPSS-D3 | −0.2 | 0.9 |
| TPSS-D3$^{ABC}$ | 0.8 | 1.2 |
| XDM+E$_9$[b] | 0.6 | 2.1 |
| PBE0-D3 | −0.6 | 1.2 |
| PBE0-D3$^{ABC}$ | 0.4 | 1.2 |
| PBE0+MBD[a] | −0.3 | 0.9 |
| HSE06-D3 | −0.7 | 1.2 |
| HSE06-D3$^{ABC}$ | 0.3 | 1.0 |

[a]Values from ref 16. [b]Values from ref 19.

The PBE-D3 functional has an MD of 1.1 kcal mol$^{-1}$ and shows a different performance for purely vdW-bound systems and hydrogen-bound systems. In Figure 2a,b are the errors for the GGA functionals depicted for the X23 set, which is separated in purely vdW-bound systems and crystals containing hydrogen bonds. The PBE-D3 functional is overbinding hydrogen-bonded crystals by 0.9 kcal mol$^{-1}$ on average. The only outlier is the nucleobase cytosine, which is underbound by 2.8 kcal mol$^{-1}$. For vdW-bound crystals PBE-D3 yields almost perfect agreement with the reference values. The largest error for these systems is found for trioxane (1.7 kcal mol$^{-1}$).

**Table 3. Reference Cohesive Energies and the Results of All Tested Methods for the X23 Test Set**

| | | | PBE | | TPSS | | HSE06 | | PBE0 | |
|---|---|---|---|---|---|---|---|---|---|---|
| | | exp.ref | -D3 | -D3$^{ABC}$ | -D3 | -D3$^{ABC}$ | -D3 | -D3$^{ABC}$ | -D3 | -D3$^{ABC}$ |
| | *vdW-Bonded Systems* | | | | | | | | | |
| 1 | 1,4-cyclohexanedione | −21.2 | −21.6 | −20.4 | −20.9 | −19.7 | −22.2 | −21.0 | −21.9 | −20.7 |
| 2 | $CO_2$ | −6.5 | −6.0 | −5.8 | −5.4 | −5.3 | −5.9 | −5.7 | −5.7 | −5.5 |
| 3 | adamantane | −16.6 | −17.1 | −15.4 | −16.7 | −14.9 | −17.8 | −16.1 | −17.0 | −15.2 |
| 4 | hexamine | −20.6 | −20.7 | −18.9 | −20.7 | −19.0 | −21.1 | −19.4 | −20.7 | −18.9 |
| 5 | trioxane | −15.9 | −14.1 | −13.3 | −13.9 | −13.2 | −13.8 | −13.0 | −13.5 | −12.8 |
| 6 | anthracene | −26.9 | −25.4 | −23.1 | −27.3 | −24.8 | −28.0 | −25.7 | −27.1 | −24.6 |
| 7 | naphthalene | −19.5 | −19.1 | −17.5 | −20.2 | −18.4 | −20.8 | −19.1 | −20.1 | −18.4 |
| 8 | benzene | −12.4 | −13.1 | −12.2 | −13.3 | −12.3 | −14.0 | −13.1 | −14.3 | −13.4 |
| 9 | pyrazine | −14.7 | −15.7 | −14.8 | −15.8 | −14.9 | −16.1 | −15.3 | −15.6 | −14.7 |
| 10 | triazine | −14.8 | −14.6 | −13.7 | −14.5 | −13.7 | −15.1 | −14.3 | −14.7 | −13.8 |
| | *H-Bonded Systems* | | | | | | | | | |
| 11 | pyrazole | −18.6 | −19.4 | −18.7 | −19.3 | −18.6 | −19.4 | −18.7 | −19.4 | −18.7 |
| 12 | imidazole | −20.8 | −22.0 | −21.3 | −21.8 | −21.1 | −22.0 | −21.3 | −21.7 | −20.9 |
| 13 | acetic acid | −17.4 | −17.2 | −16.7 | −16.3 | −15.8 | −17.0 | −16.5 | −16.8 | −16.2 |
| 14 | ammonia | −8.9 | −10.3 | −10.1 | −9.4 | −9.2 | −9.8 | −9.6 | −10.6 | −10.4 |
| 15 | cyanamide | −19.1 | −22.4 | −22.0 | −21.6 | −21.2 | −21.4 | −21.0 | −22.1 | −21.7 |
| 16 | cytosine | −40.6 | −37.8 | −36.5 | −38.1 | −36.7 | −38.3 | −37.0 | −37.9 | −36.5 |
| 17 | ethylcarbamate | −20.6 | −21.4 | −20.7 | −20.8 | −20.0 | −21.2 | −20.4 | −21.0 | −20.3 |
| 18 | formamide | −18.9 | −20.1 | −19.7 | −19.7 | −19.2 | −19.9 | −19.5 | −19.9 | −19.5 |
| 19 | oxalic acid ($\alpha$) | −23.0 | −23.0 | −22.2 | −22.0 | −21.3 | −22.8 | −22.1 | −24.4 | −23.6 |
| 20 | oxalic acid ($\beta$) | −23.0 | −23.7 | −22.9 | −22.8 | −22.1 | −23.7 | −23.0 | −23.6 | −22.9 |
| 21 | succinic acid | −31.1 | −32.0 | −30.8 | −30.9 | −29.8 | −31.9 | −30.7 | −31.7 | −30.5 |
| 22 | uracil | −32.4 | −33.5 | −32.4 | −33.7 | −32.6 | −34.3 | −33.1 | −33.7 | −32.5 |
| 23 | urea | −24.5 | −27.3 | −26.7 | −26.6 | −26.0 | −27.3 | −26.7 | −27.5 | −26.9 |


dx.doi.org/10.1021/jp501237c | J. Phys. Chem. C 2014, 118, 7615−7621

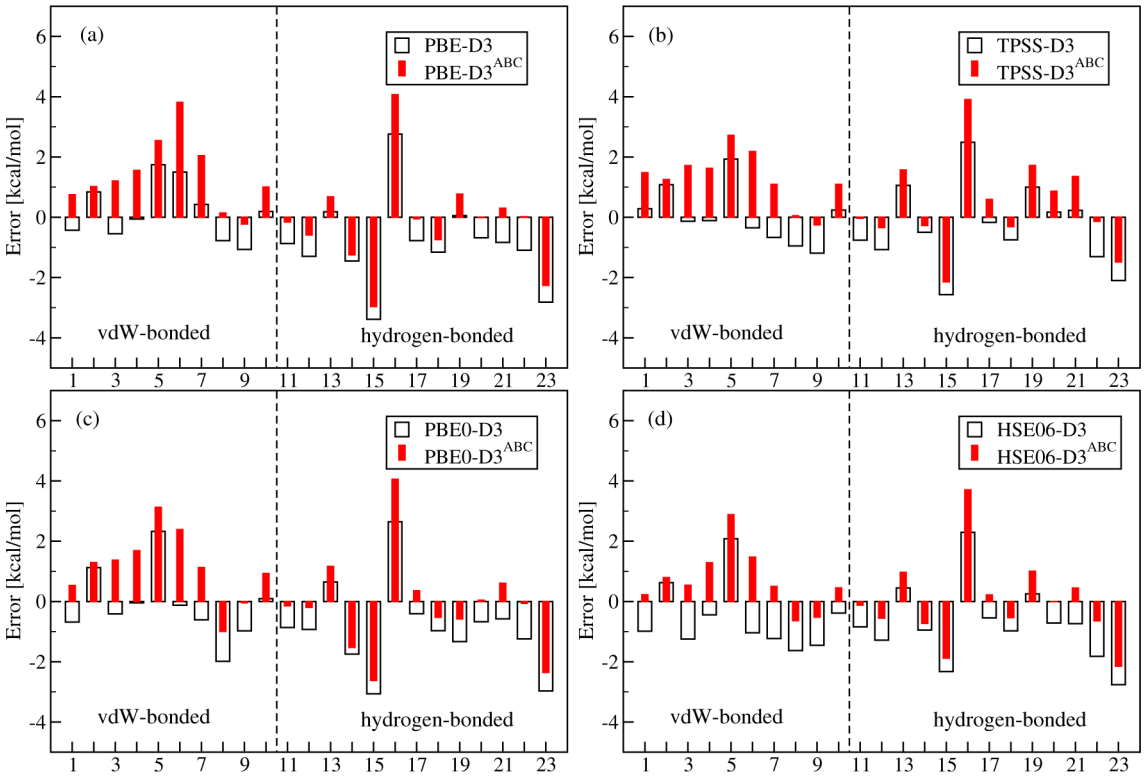


**Figure 2.** Deviations of the dispersion-corrected GGA functionals PBE (a) and TPSS (b) and hybrid functionals PBE0 (c) and HSE06 (d) for the X23 set.

Adding the three-body-contribution to the dispersion energy shifts the MD from −0.4 to 0.7 kcal mol$^{-1}$, and the MAD increases slightly from 1.1 to 1.2 kcal mol$^{-1}$. A similar behavior has been observed in a previous work on the binding energies of supramolecular complexes[9] with PBE-D3.

Statistically better results are found for the metaGGA TPSS. This functional does not show the tendency to overbind H-bond-dominated systems; therefore, a very small MD of only −0.2 kcal mol$^{-1}$ is achieved, and the MAD is the lowest of all tested methods. Adding the three-body dispersion energy increases the MD to a positive (underbinding) value of 0.8 kcal mol$^{-1}$.

The hybrid functionals PBE0-D3 and HSE06-D3 show more overbinding tendency. In Figure 2c,d the errors of the hybrid functionals are shown. For PBE0-D3, the MAD is very similar to that of the PBE functional, and also similarly, the purely vdW-bound systems are described better. The inclusion of the three-body term improves the MD to a small positive value of 0.4 kcal mol$^{-1}$. The MAD stays unaltered for PBE0-D3$^{ABC}$. For the range-separated hybrid functional HSE06-D3 an improvement by the three-body term is observed. The overbinding tendency of HSE06-D3 is corrected, and a very small MD of 0.3 kcal mol$^{-1}$ and MAD of 1.0 kcal mol$^{-1}$ are obtained.

For a few cases (cytosine, trioxane), a significant underbinding of 3−4 kcal mol$^{-1}$ is observed for all functionals. This underbinding is reinforced by the three-body term, which is always repulsive for crystals. This deterioration may result from neglecting higher-order terms in the dispersion interaction, which are canceled in the other cases by, e.g., short-range effects or due to symmetry or are too small. The importance of of these terms which are partially implicitely included in D3 by the short-range damping parametrization is investigated for larger systems in ref 36.

**Cell Volumes.** In addition to the energies, Otero-dela-Rosa et al. proposed reference values for structural properties of the organic crystals and an approximation to include the expansion caused by vibrational effects in normal geometry optimizations. In this treatment the systems are optimized at a negative external pressure equal to the so-called "thermal pressure", which is calculated from the vibrational energies at different volumes.[14] These thermal pressures were published for the 21 crystals in the C21 benchmark set and are used here to optimize the crystals with the DFT-D3 method. The two additional systems from the X23 set, hexamine and succinic acid (no. 4 and 21), are missing in this part of the set.

A convenient but also sensitive comparison between theory and experiment concerns the volume of the unit cell since a systematic error in the lattice constants scales cubically for the volume. While intramolecular bond lengths are not very sensitive to the applied theoretical level (for a detailed recent discussion and examples with and without dispersion correction see ref 37), unit cell parameters depend strongly on the dispersion correction.

First we compare the obtained unit cell volumes in standard optimizations, which do not include the approximated expansions due to thermal and zero-point vibrations. There is one noteworthy outlier in the set. The unit cell of $CO_2$ is computed 12% too large by TPSS-D3, while the volume of nearly all other systems is underestimated. This large deviation was already observed by Johnson and Tkatchenko.[14,16] We note that the same misbehavior of the D3 correction for this case is also observed with other dispersion corrections (XDM or vdW-TS), and hence for the discussion and statistics we exclude this outlier from the set.

For the structures with no thermal correction, one would expect too small computed lattice constants and volumes which


dx.doi.org/10.1021/jp501237c | J. Phys. Chem. C 2014, 118, 7615−7621

is indeed found. Table 5 shows that both functionals have negative percentage MD values. PBE-D3 underestimates the volumes by about 1% and TPSS-D3 by about 2%. This is in good agreement with the estimated expansion caused by zero-point vibrations of about 1.5% for simple systems.[16] In Figure 3 are the relative deviations of the calculated volumes from the measured X-ray references for the TPSS-D3 functional with and without the three-body term depicted. For the vdW-bonded systems, TPSS-D3 shows a higher tendency to underestimate the unit cell volumes, compared to the hydrogen-bound systems. All cell volumes of the vdW-bonded systems, but $CO_2$ and trioxane, are underestimated. One can see that the three-body term, which is repulsive for all solid systems, increases the volumes of the unit cells. This shift to larger unit cells is very small and also quite constant for all systems considered. On average the volume is increased by 0.8% (with a standard deviation of 0.3%).

**Table 5. Statistical Results for the Cell Volumes of 20 Organic Molecules[a]**

| | M%D | MA%D |
|---|---|---|
| Without External Pressure | | |
| PBE-D3 | −1.1 | 1.3 |
| TPSS-D3 | −2.3 | 2.7 |
| TPSS-D3$^{ABC}$ | −1.5 | 2.2 |
| With External Pressure | | |
| PBE-D3 | 1.2 | 2.1 |
| TPSS-D3 | 2.1 | 3.2 |
| B86b-XDM[b] | 3.8 | 3.8 |

[a]Values are in %. [b]Ref 14.

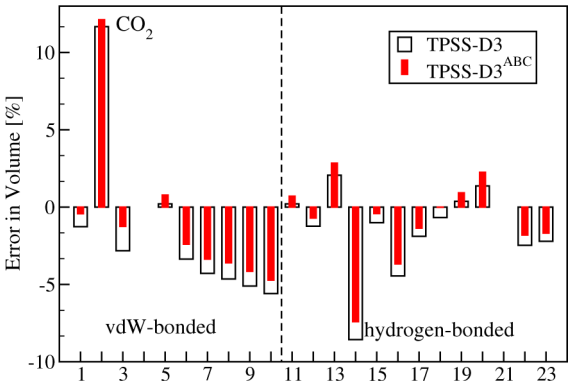


**Figure 3.** Relative deviations of the unit cell volumes for the 23 organic molecules.

The optimization with the thermal pressure applied as a negative external pressure during the optimization results in an expansion of the cells. For PBE-D3 the cell volumes in comparison to the experimental data are now overestimated by about 1% on average, and TPSS-D3 has an average error of 2%. This finding is consistent with the observations in ref 37 that PBE-D3 and TPSS-D3 already overestimate the size (volumes) of isolated molecules by about 1.3%. The unsigned relative error (MA%D) becomes larger for the thermally corrected optimizations. In essence the error of the GGA functional partially cancels out the error introduced by disregarding vibrational effects. With this error cancellation, the average deviation from X-ray volumes is less than 3% which translates to an average error of about 1% in the lattice constants. At this point we want to stress that for this accuracy a very large basis set and tight optimization convergence criteria are required.

## CONCLUSIONS

We have shown that DFT-D3 with various approximate density functionals provides accurate results for the cohesive energies of organic and rare gas crystals. The error of all tested methods is close to the uncertainty of the reference values which was estimated to be about 0.7 kcal mol$^{-1}$. The application of computationally more demanding hybrid functionals leads to only small or no improvements. This is similar to noncovalently interacting molecules where GGAs and hybrids perform similarly as well.[38,39] The comparison with the results of other dispersion corrections from the literature shows that all yield very similar high accuracy with only small differences in their performance.

The three-body dispersion interaction term does not improve the results on a GGA level. Similar observations were also made for supramolecular complexes.[9] However, an improvement in the performance is found for HSE06-D3$^{ABC}$. Presumably on a GGA level there is some incorrect short-range many-body correlation treatment by the density functional[40] which is improved at a higher hybrid level. In general we recommend to add the three-body energy since it has a good physical basis and improves the results of higher-level functionals. The inclusion of this term for optimizations can be disregarded since the effects are negligible for almost all practical purposes.

Furthermore, we have tested the dispersion correction for geometric properties. Unit cell volumes are reproduced very well by DFT-D3. Neglecting vibrational effects results in an underestimation of 1−2% of computed volumes. Approximating these effects results in a systematic overestimation of 1−2% of the volumes by (meta)GGAs which is consistent with the estimated inherent error of these functionals, which tend to overestimate isolated (organic) molecule "volumes" (as, e.g., measured by rotational constants) by about 1.3%. In summary our study shows that the future of dispersion-corrected DFT calculations for organic (or in general insulator) systems is bright and can lead to a more quantitative understanding of an important state of matter.

## ASSOCIATED CONTENT

### Supporting Information

Table S1 in contains the experimental and calculated cell parameters for the 20 tested molecular crystals. This material is available free of charge via the Internet at http://pubs.acs.org.

## AUTHOR INFORMATION

### Corresponding Author

*E-mail: grimme@thch.uni-bonn.de.

### Notes

The authors declare no competing financial interest.

## REFERENCES

(1) Pérez-Jordá, J. M.; Becke, A. D. A Density-Functional Study of van der Waals Forces: Rare Gas Diatomics. *Chem. Phys. Lett.* **1995**, *233*, 134−137.

(2) Kristyán, S.; Pulay, P. Can (semi)local Density Functional Theory Account for the London Dispersion Forces? *Chem. Phys. Lett.* **1994**, *229*, 175−180.

(3) Hobza, P.; Šponer, J.; Reschel, T. Density Functional Theory and Molecular Clusters. *J. Comput. Chem.* **1995**, *16*, 1315−1325.
(4) Grimme, S. Density Functional Theory with London Dispersion Corrections. *WIREs Comput. Mol. Sci.* **2011**, *1*, 211−228.
(5) Vydrov, O. A.; Van Voorhis, T. Nonlocal van der Waals Density Functional: The Simpler the Better. *J. Chem. Phys.* **2010**, *133*, 244103.
(6) Tkatchenko, A.; DiStasio, R. A.; Car, R.; Scheffler, M. Accurate and Efficient Method for Many-Body van der Waals Interactions. *Phys. Rev. Lett.* **2012**, *108*, 236402.
(7) Otero-de-la Roza, A.; Johnson, E. R. Van der Waals Interactions in Solids using the Exchange-Hole Dipole Moment Model. *J. Chem. Phys.* **2012**, *136*, 174109.
(8) Grimme, S.; Antony, J.; Ehrlich, S.; Krieg, H. A Consistent and Accurate Ab Initio Parametrization of Density Functional Dispersion Correction (DFT-D) for the 94 Elements H-Pu. *J. Chem. Phys.* **2010**, *132*, 154104.
(9) Risthaus, T.; Grimme, S. Benchmarking of London Dispersion-Accounting Density Functional Theory Methods on Very Large Molecular Complexes. *J. Chem. Theory Comput.* **2013**, *9*, 1580−1591.
(10) Řezáč, J.; Riley, K. E.; Hobza, P. S66: A Well-balanced Database of Benchmark Interaction Energies Relevant to Biomolecular Structures. *J. Chem. Theory Comput.* **2011**, *7*, 2427.
(11) Bardwell, D. A.; Adjiman, C. S.; Arnautova, Y. A.; Bartashevich, E.; Boerrigter, S. X. M.; Braun, D. E.; Cruz-Cabeza, A. J.; Day, G. M.; Della Valle, R. G.; Desiraju, G. R.; et al. Towards Crystal Structure Prediction of Complex Organic Compounds − a Report on the Fifth Blind Test. *Acta Crystallogr., Sect. B* **2011**, *67*, 535−551.
(12) Marom, N.; DiStasio, R. A.; Atalla, V.; Levchenko, S.; Reilly, A. M.; Chelikowsky, J. R.; Leiserowitz, L.; Tkatchenko, A. Many-Body Dispersion Interactions in Molecular Crystal Polymorphism. *Angew. Chem., Int. Ed.* **2013**, *52*, 6629−6632.
(13) Bučko, T.; Hafner, J.; Lebègue, S.; Ángyán, J. G. Improved Description of the Structure of Molecular and Layered Crystals: Ab Initio DFT Calculations with van der Waals Corrections. *J. Phys. Chem. A* **2010**, *114*, 11814.
(14) Otero-de-la Roza, A.; Johnson, E. R. A Benchmark for Non-Covalent Interactions in Solids. *J. Chem. Phys.* **2012**, *137*, 054103.
(15) Reilly, A. M.; Tkatchenko, A. Seamless and Accurate Modeling of Organic Molecular Materials. *J. Phys. Chem. Lett.* **2013**, *4*, 1028−1033.
(16) Reilly, A. M.; Tkatchenko, A. Understanding the Role of Vibrations, Exact Exchange, and Many-Body van der Waals Interactions in the Cohesive Properties of Molecular Crystals. *J. Chem. Phys.* **2013**, *139*, 024705.
(17) Axilrod, B. M.; Teller, E. Interaction of the van der Waals Type Between Three Atoms. *J. Chem. Phys.* **1943**, *11*, 299−300.
(18) Muto, Y. *Proc. Phys. Math. Soc. Jpn.* **1944**, *17*, 629.
(19) Otero-de-la Roza, A.; Johnson, E. R. Many-Body Dispersion Interactions from the Exchange-Hole Dipole Moment Model. *J. Chem. Phys.* **2013**, *138*, 054103.
(20) Schatschneider, B.; Monaco, S.; Tkatchenko, A.; Liang, J.-J. Understanding the Structure and Electronic Properties of Molecular Crystals Under Pressure: Application of Dispersion Corrected DFT to Oligoacenes. *J. Phys. Chem. A* **2013**, *117*, 8323−8331.
(21) Bučko, T.; Lebègue, S.; Hafner, J.; Ángyán, J. G. Tkatchenko-Scheffler van der Waals Correction Method With and Without Self-consistent Screening Applied to Solids. *Phys. Rev. B* **2013**, *87*, 064110.
(22) Reckien, W.; Janetzko, F.; Peintinger, M. F.; Bredow, T. Implementation of Empirical Dispersion Corrections to Density Functional Theory for Periodic Systems. *J. Comput. Chem.* **2012**, *33*, 2023−2031.
(23) Bučko, T.; Lebégue, S.; Hafner, J.; Ángyán, J. G. Improved Density Dependent Correction for the Description of London Dispersion Forces. *J. Chem. Theory Comput.* **2013**, *9*, 4293−4299.
(24) Johnson, E. R.; Becke, A. D. A Post-Hartree-Fock Model of Intermolecular Interactions: Inclusion of Higher-Order Corrections. *J. Chem. Phys.* **2006**, *124*, 174104.
(25) Grimme, S.; Ehrlich, S.; Goerigk, L. Effect of the Damping Function in Dispersion Corrected Density Functional Theory. *J. Comput. Chem.* **2011**, *32*, 1456.
(26) Koide, A. A New Expansion for Dispersion Forces and its Application. *J. Phys. B* **1976**, *9*, 3173.
(27) Kresse, G.; Furthmüller, J. Efficient Iterative Schemes for Ab Initio Total-Energy Calculations using a Plane-Wave Basis Set. *Phys. Rev. B* **1996**, *54*, 11169−11186.
(28) Blöchl, P. E. Projector Augmented-Wave Method. *Phys. Rev. B* **1994**, *50*, 17953.
(29) Kresse, G.; Joubert, J. From Ultrasoft Pseudopotentials to the Projector Augmented-Wave Method. *Phys. Rev. B* **1999**, *59*, 1758.
(30) Perdew, J. P.; Burke, K.; Ernzerhof, M. Generalized Gradient Approximation Made Simple. *Phys. Rev. Lett.* **1996**, *77*, 3865.
(31) Tao, J.; Perdew, J. P.; Staroverov, V. N.; Scuseria, G. E. Climbing the Density Functional Ladder: Nonempirical Meta Generalized Gradient Approximation Designed for Molecules and Solids. *Phys. Rev. Lett.* **2003**, *91*, 146401.
(32) Adamo, C.; Barone, V. Toward Reliable Density Functional Methods Without Adjustable Parameters: The PBE0Model. *J. Chem. Phys.* **1999**, *110*, 6158−6170.
(33) Krukau, A. V.; Vydrov, O. A.; Izmaylov, A. F.; Scuseria, G. E. Influence of the Exchange Screening Parameter on the Performance of Screened Hybrid Functionals. *J. Chem. Phys.* **2006**, *125*, 224106.
(34) Paier, J.; Marsman, M.; Hummer, K.; Kresse, G.; Gerber, I. C.; Ángyán, J. G. Screened Hybrid Density Functionals Applied to Solids. *J. Chem. Phys.* **2006**, *124*, 154709.
(35) Murnhagan, F. D. The Compressibility of Media under Extreme Pressures. *Proc. Natl. Acad. Sci. U.S.A.* **1944**, *30*, 244.
(36) Ambrosetti, A.; Alfè, D.; DiStasio, R. A.; Tkatchenko, A. Hard Numbers for Large Molecules: Toward Exact Energetics for Supramolecular Systems. *J. Phys. Chem. Lett.* **2014**, *5*, 849−855.
(37) Grimme, S.; Steinmetz, M. Effects of London Dispersion Correction in Density Functional Theory on the Structures of Organic Molecules in the Gas Phase. *Phys. Chem. Chem. Phys.* **2013**, *15*, 16031−16042.
(38) Goerigk, L.; Kruse, H.; Grimme, S. Benchmarking Density Functional Methods against the S66 and S66 × 8 Datasets for Non-Covalent Interactions. *ChemPhysChem* **2011**, *12*, 3421−3433.
(39) Goerigk, L.; Grimme, S. A Thorough Benchmark of Density Functional Methods for General Main Group Thermochemistry, Kinetics, and Noncovalent Interactions. *Phys. Chem. Chem. Phys.* **2011**, *13*, 6670−6688.
(40) Tkatchenko, A.; von Lilienfeld, O. A. Popular Kohn-Sham Density Functionals Strongly Overestimate Many-Body Interactions in van der Waals Systems. *Phys. Rev. B* **2008**, *78*, 045116.